Available online at www.sciencedirect.com
SCIENCE DIRECT®
Journal of volcanology and geothermal research
ELSEVIER
Journal of Volcanology and Geothermal Research xx (2006) xxx–xxx
www.elsevier.com/locate/jvolgeores

Textural effects of steady state behaviour of the Stromboli feeding system

Pietro Armienti [a,*], Lorella Francalanci [b], Patrizia Landi [c]

[a] *Dipartimento di Scienze della Terra, Pisa University, Via S. Maria 53, 56126 Pisa, Italy*
[b] *Dipartimento di Scienze della Terra, Via G. La Pira 4. I50121 Firenze, Italy*
[c] *Istituto Nazionale di Geofisica e Vulcanologia, Via della Faggiola 32, 56126 Pisa, Italy*

Received 4 July 2005; received in revised form 30 March 2006; accepted 9 May 2006

Abstract

The exceptionally persistent activity of Stromboli volcano has lasted for at least 1400 years. The normal strombolian activity is periodically interrupted by more energetic explosions (1–2 per year) and by sporadic effusive episodes (every 10–20 years). Normal activity and effusive episodes are characterized by crystal-rich high-K to shoshonitic basalts issuing from a volatile-poor shallow system. Crystal-poor pumice are emitted only during more violent explosions, and are thought to derive from deep pulses of volatile-rich magma. Shallow level degassing induces massive crystallization of deep pulses of feeding magma that, continuously mixing with the resident one, produces the crystal-rich shoshonite of the persistent activity. We examined the crystallization history of the crystal-rich, shallow reservoir using plagioclase Crystal Size Distribution (CSD) analysis of scoriae and lavas emitted in the past twenty years. CSDs show a linear dependence from crystal size in the size interval 0.06–1.2 mm; number density of larger crystals is biased by right hand truncation effects. CSDs slopes and intercepts are quite constant during the whole considered time span revealing a system that is close to the equilibrium also from a kinetic point of view. The linear crystal size distribution are reached by the system through episodes of growth and resorption, respectively occurring in the degassed and undegassed magma during the continuous mixing in the feeding system. Plagioclase net growth rate ($2*10^{-11}$ cm/s) results from a balance of growth (10^{-10} cm/s) and resorption episodes which induce spectacular zoning and resorption textures in crystals larger than 200 μm. CSDs of mafic phases cannot be accurately acquired on each single sample due to poor counting statistics; the evaluation of pyroxene and olivine CSD on the whole data set, however, confirms the conclusions acquired from plagioclase CSDs.
© 2006 Published by Elsevier B.V.

Keywords: crystal size distribution; plagioclase growth; magma residence time

1. Introduction

Mass balance calculations often allow the description of evolutionary processes occurring in shallow level magma reservoirs, where numerous and complex phenomena affect magma during crystallisation. Processes varying from simple fractional crystallisation to refilling+tapping (RFT) and possible accumulation and recycling of crystals may be modelled by means of mass balance calculations evaluating partitioning of major and trace elements between liquid and solid fractions of magma in the feeding system. All the mechanisms acting on elemental distributions between solids and liquid must leave a trace in the modal composition of magmas that can be quantitatively evaluated in order to test hypotheses and conclusions

* Corresponding author.
E-mail address: armienti@dst.unipi.it (P. Armienti).

0377-0273/$ - see front matter © 2006 Published by Elsevier B.V.
doi:10.1016/j.jvolgeores.2006.05.004

UNCORRECTED PROOF

ARTICLE IN PRESS

drawn on the basis of geochemical data. In fact, mass balance calculations generally satisfy a set of equations that describe the situation at the end of the process and in general do not prove that the hypothesised mechanism was acting, they simply state that a given process is a possible one. Modal data, in this frame, can provide a tool to test petrogenetic models based on geochemical data, since the development of a distribution of crystals in a magma should obey a set of kinetic and physical conditions satisfying a different and independent set of equations.

In this context, Stromboli, a stratovolcano of the Aeolian island arc, Southern Tyrrhenian Sea, Italy, represents a well studied system that has been erupting in practically steady state conditions since a period between the third and the seventh century A.D. (Giberti et al., 1992; Francalanci et al., 1993, 2004; Rosi et al., 2000). Stromboli is well known by volcanologists for its exceptional persistence of volcanic activity, which consists of intermittent mild explosions ejecting ash, scoriaceous bombs and lapilli, at an interval of about 10–20 min. This normal activity is periodically interrupted by more energetic explosions (major explosion or paroxysms), on average 2–3 per year in the last decade, and episodes of lava emission (every 4 years in the past 120 years) (Barberi et al., 1993; Bertagnini et al., 1999). Two types of magma, mainly differing in crystal and volatile contents, have fed the volcano since the beginning of its persistent activity: a highly porphyritic magma (HP-magma), erupted as scoriaceous bombs, lapilli and lavas during the normal activity and effusive episodes, and a volatile-rich, aphyric to slightly porphyritic magma, with low phenocryst contents (LP-magma), which is emitted as pumices only during paroxysms. The latter is usually mingled with the HP-magma, mainly due to syn-eruptive processes (Bonaccorso et al., 1996; Bertagnini et al., 1999; Francalanci et al., 1999; Rosi et al., 2000).

The HP-magmas are high-K shoshonitic basalts with a phenocryst content of ~50 vol.% and a volatile content 0.60 wt.%. The LP-magmas are slightly less evolved high-K basalts, with lower silica and K_2O contents than the HP-magmas (SiO_2 48.2–49.2 wt.% and 48.6–51.5 wt.%, and K_2O 1.5–2 wt.% and 2–2.5 wt.%, respectively — Fig. 1). They show a crystal content <5% vol, with high volatile contents ~~between~~ 1.8 ~~and~~ 3.4 wt.% (Métrich et al., 2001). The HP-magmas have slightly higher incompatible trace element contents, except for Sr, and lower MgO and compatible trace element abundances than LP-magmas (Francalanci et al., 2004).

Sr isotope ratios of the HP-magmas from the beginning of the 20th century to around 1980 are constant with an average of 0.70626 (±2, 2σ). After 1980, $^{87}Sr/^{86}Sr$ smoothly decreases to a value of 0.70615 in the 2003 scoria. The pumice samples (LP-magmas) have significantly lower Sr isotope ratios than scoria, with $^{87}Sr/^{86}Sr \approx 0.70610$. Nd isotope ratios of scoria, lavas and pumice are more homogeneous (0.51256±1) (Francalanci et al., 1999, 2004).

Volatile-rich magmas are thought to originate in the lower part of the plumbing system, whereas HP-magmas are associated with a shallow reservoir and result from the crystallisation of the LP-magma, mainly driven by decompression and water loss at low pressure, associated with minor crystal fractionation and recycling of old crystals. The latter are brought into the shallow reservoir by the replenishing LP magma (Francalanci et al., 1999, 2004, 2005; Métrich et al., 2001; Bertagnini et al., 2003; Vagelli et al., 2003; Landi et al., 2004).

The thermal and gas budgets and the homogeneous composition of the erupted rocks allow one to consider the present shallow plumbing system of the volcano in a steady-state condition, which agrees with the presence of an open conduit system and nearly continuous eruptions (Giberti et al., 1992; Allard et al., 1994, ~~2000~~; Harris and Stevenson, 1997; Francalanci et al., 1999, 2004; Rosi et al., 2000). Accordingly, the dynamics of the shallow magmatic system has been envisioned as a steady state, continuously erupting and crystallising magma chamber that is replenished at a constant rate by the LP-magma. Mixing and olivine+clinopyroxene+plagioclase crystallisation control the evolution of the magmas feeding the present-day activity of Stromboli. The temporal decrease of Sr isotope ratios in scoria and lavas starting from 1980 is a fundamental piece of evidence for continuous mixing beginning around 1980, the shallow

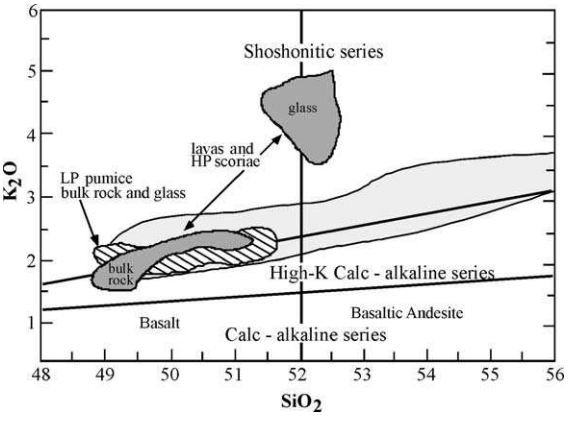


Fig. 1. Composition of Stromboli products ~~analysed in this work~~. The light grey field indicates the composition of shoshonitic products of the island. LP: with low phenocryst content; HP highly porphyritic.

UNCORRECTED PROOF

HP-magma reservoir was fed by magma with a different and lower Sr isotope signature. This replenishment brought the shallow magmatic system towards a new isotopic equilibrium condition.

Through the application of a time series analysis to the decrease of Sr isotope ratios starting around 1980, a short residence time has been calculated (≈19 years) for the magma feeding the volcanic activity at Stromboli. This calculation is based on the assumption that the shallow reservoir is chemically homogeneous (i.e., magma mixing time is shorter than magma residence time) and there are no time dependent variations in Sr contents, as demonstrated by the homogeneous compositions of lavas and scoria erupted during the last century and by its constant Sr contents (Francalanci et al., 1999). In this paper we examine the crystallization history of the HP-magma using Crystal Size Distributions of minerals in a set of crystal-rich scoriae and lavas erupted at Stromboli over

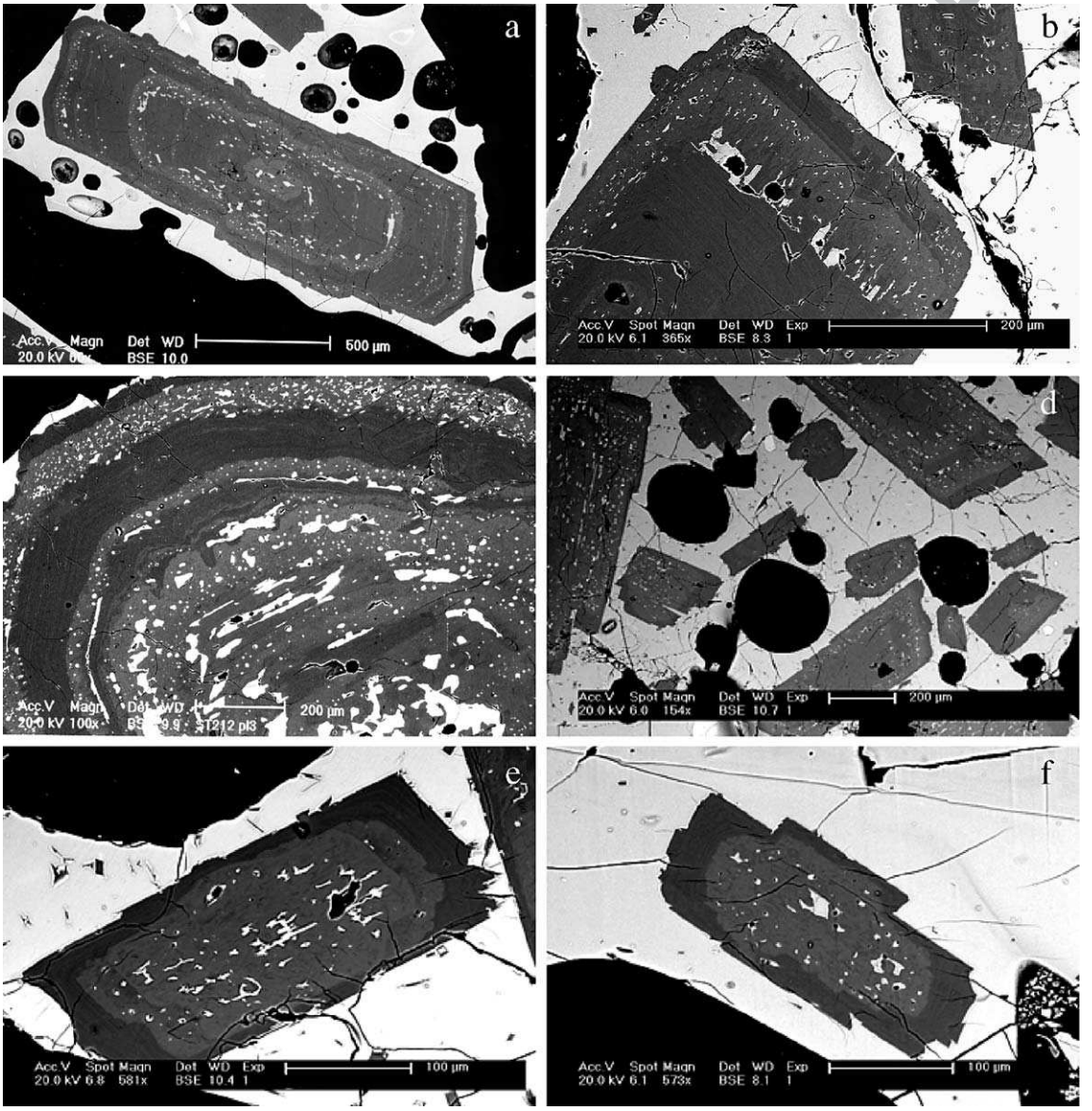


Fig. 2. Back-scattered electron images of plagioclase phenocrysts. (a) Characteristic zoning of the plagioclase, consisting of alternating layers of labradorite (dark grey) and sieve-textured, bytownite (clear grey). (b) Enlargement showing small-scale (1–5 µm) oscillatory zoning in labradoritic layers and sieved textures with abundant glass inclusions in bytownitic layers. A dissolution surface which indents for several tens of µm a labradoritic layer is evident in the external part. (c) Dissolution events can dissolve up to 150–200 µm of labradoritic layers. (d) Crystals larger than ~200 µm have alternating zoning with dissolution surfaces, whereas dissolution surfaces are not present in crystals <200–250 µm (see f). (e) crystal ~330×130 µm showing one dissolution event. (f) crystals <200–250 frequently show a sharp zoning between bytownitic core and labradoritic rim.

ARTICLE IN PRESS

the past two decades. These samples have been taken as representative of a period of activity, during which a detailed sampling was performed with time. The final goal of the paper is to use present-day Stromboli plumbing system as an end-member example of a steady state crystallizing system.

2. Petrography

Detailed petrographic accounts of the products of the recent activity of Stromboli are reported in numerous papers (Francalanci et al., 1993, 2004; Métrich et al., 2001; Landi et al., 2004). Apparently a pure LP-magma end-member has never been erupted due to widespread mingling with the crystal-rich resident magma. The less mingled crystal-poor pumices have phenocryst contents lower than 10% and lack plagioclase phenocrysts. Equilibrium mafic phases of LP-magmas have Mg# higher than olivine and clinopyroxene of HP-magmas.

HP lavas and scoriae have Porphyritic Index of about 45–55 vol.% with seriated crystals of plagioclase, clinopyroxene and olivine. Clinopyroxene crystals may

UNCORRECTED PROOF

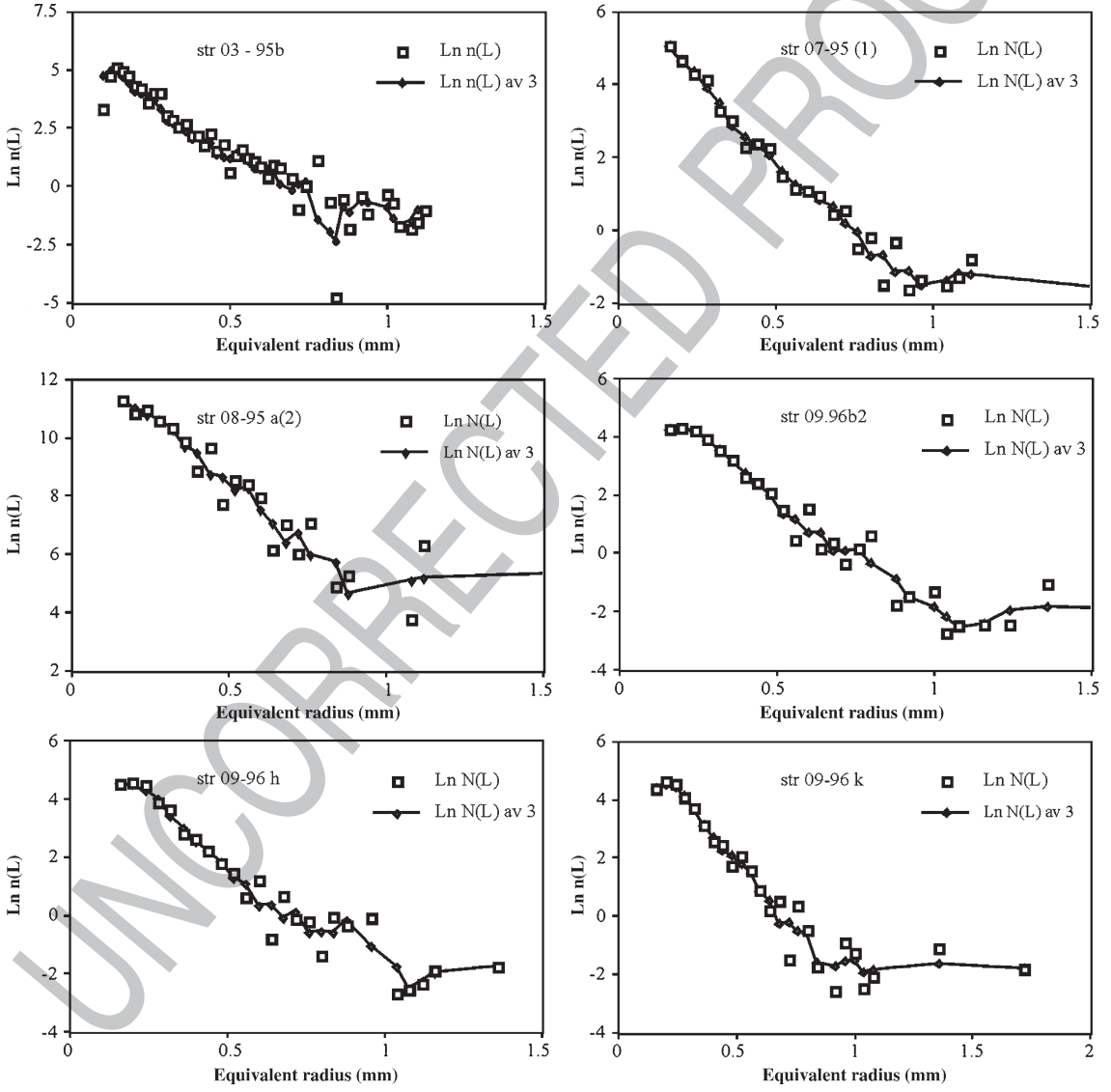


Fig. 3. Selected plagioclase Crystal Size Distribution in Stromboli ~~lava~~. Data are shown in semi-logarithmic diagrams vs. the size of the grain. Size is assumed equal to the radius of the circle whose area is equivalent to the area of the mineral in the section. Equivalent radii in mm. Number densities $n(L)$ in mm^{-4}. Sample number is referred in the figure. Continuous lines join smoothed data calculated on the average of three contiguous points (av 3). For size larger than about 1.2 mm Eq. (1) is not fulfilled and there is an apparent decrease of CSD slopes.

ARTICLE IN PRESS

be as large as 5 mm, with composition varying from Mg# 0.71 and Mg# 0.91 and a mode at Mg# 0.75–0.77. The diopsidic composition is found as resorbed cores and/or thin intermediate zones. Olivine generally occurs as euhedral crystals up to 3–4 mm wide, and shows uniform composition, of Fo70–73. Glomeroporphyritic aggregates are commonly found in these rocks and are mainly composed of clinopyroxene and clinopyroxene+olivine, with small interstitial plagioclase. Plagioclase phenocrysts, the most abundant phase (27–37 vol.%), have lengths of up to 2 mm and show a typical concentric zoning consisting of alternating layers of An60–An70 and An70–90 (dark and light grey respectively in Fig. 2). An60–70 zones exhibit ubiquitous, small-scale (1–5 μm) oscillatory zoning, whereas An70–90 bands are sieve-textured, patchy-zoned. (Fig. 2a and b). Euhedral rims attain labradoritic composition in equilibrium with the groundmass (An65–70). Detailed inspection of SEM images reveals that bytownitic layers frequently grow on dissolution surfaces, mainly involving labradoritic zones, which can indent layers from a few up to 150–200 μm (Fig. 2b and c). Alternating zoning with corroded layers occur in crystals larger than 250–300 μm (Fig. 2d,e). In contrast, crystals between 100 and 200 μm lack dissolution events and may only show a sharp jump from bytownite core to a labradorite rim (Fig. 2f).

t1.1 Table 1
t1.2 List of sample and data on vesicularity and crystal content

t1.3 Sample	Area	Vescicularity	Detected crystals ($0.2<R<5$ mm)		
t1.4 Date	mm^2	%	Plagioclase	Clinopyroxene	Olivine
t1.5 str45(04/84)	649	50	2021		
t1.6 str7-94	505	57	923	23	13
t1.7 str9-94-B1	486	44	1270	56	22
t1.8 str9-94-B2	394	47	1027	42	16
t1.9 str09-94-A	499	42	1553	28	
t1.10 str95a(03/95a)	533	48	1549	39	22
t1.11 str95b(03/95b)	631	31	2012	83	20
t1.12 str95c(03/95c)	661	31	2347	60	34
t1.13 str07-95(2)	558	41	1721	58	24
t1.14 str08-95 b(1)	504	49	1230	37	26
t1.15 str08-95-a(1)	560	64	725	31	9
t1.16 str08-95-a(2)	518	65	965	21	16
t1.17 str07-95(1)	570	37	1591	57	37
t1.18 str09-95 a(1)	617	47	1419	48	19
t1.19 str09-95 a(2)	637	52	1426	46	28
t1.20 str09-95 b	663	41	1965	46	43
t1.21 str09-95 c(1)	663	51	1572	42	23
t1.22 str09-95 c(2)	471	54	953	45	37
t1.23 str09-95-b(2)	466	65	967	32	32
t1.24 str04-96 a1	549	29	1505	65	31
t1.25 str04-96 a2	355	35	1222	26	11
t1.26 str04-96 b	682	40	1865	64	32
t1.27 str08-96 b	682	48	1401	52	23
t1.28 str09-96	682	35	1808	72	30
t1.29 str09-96 a	682	35	1701	66	
t1.30 str09-96 b1	665	35	1609	55	
t1.31 str09-96 b2	675	35	1656	58	
t1.32 str09-96 e1	682	51	1465	41	33
t1.33 str09-96 f1	682	35	1654	73	36
t1.34 str09-96 f2	662	35	1695	49	27
t1.35 str09-96 h	682	35	1777	49	
t1.36 str09-96 l	653	35	1348	31	
t1.37 str09-96-i	682	35	1606	43	
t1.38 str09-96-j	637	35	1754	70	
t1.39 str09-96-k	659	35	1841	65	
t1.40 STR29.12.02	1720	19	6555		
t1.41 STR15.01.03	2240	27	8930		
t1.42 STR26.06.03	1414	27	5247		

t1.43 *: scoriaceous block.
t1.44 **: lava.

UNCORRECTED PROOF

ARTICLE IN PRESS

Dissolution events have been explained as being due to inputs of volatile-rich magma from the deeper portion of the plumbing system, into the volatile-poor, crystal-rich body (Landi et al., 2004). Plagioclase, growing in equilibrium in the volatile-poor magma, can be admixed in LP magma whose high H_2O content induces plagioclase resorption. Subsequent degassing rapidly restores the plagioclase stability field, inducing growth of sieve-textured Ca-rich layers and nucleation of bytownitic plagioclase which forms the cores of new crystals (e.g. Fig. 2f). Nevertheless not all the phenocryst cores appear to have the same origin. In fact, some resorbed cores have been linked to recycling of old crystals on the basis of their higher Sr isotope ratios with respect to the external zones. These nuclei probably derived from an old cumulus crystal mush zone and are transported into the shallow reservoir by the replenishing LP magma (Francalanci et al., 2005).

3. Crystal size distributions

3.1. Collection of data

Crystal Size Distributions (CSDs) were measured on 32 rock samples of the past two decades of activity. 28 samples are scoria and scoriaceous blocks related to the explosive activity of the period July 1994 to September 1996, during which a detailed sampling of the erupted products was available. Scoriaceous angular blocks represent scoriae forming the upper part of the crater rim which are disrupted by a following explosive eruption. Based on the freshness of these rocks (only olivine oxidation is sometimes present) and considering the high alteration power of the crater rim environment (hot and acid gases are crossing these rocks), it is reasonable to suppose that these scoriae were erupted a short time before sampling. The sample STR45 is a scoria from the normal Strombolian activity of April 1984, chosen to investigate the same activity in a previous period. The samples STR29.12.02, STR15.01.03 and STR26.06.03 are lavas from the 2002–2003 effusive event, taken for comparison with the scoria samples.

Modal data of this study are reported as CSDs (Fig. 3), defined as the number, per unit volume and unit size, of crystals of given linear dimension L (Marsh, 1988; Cashman and Marsh, 1988; Maaloe et al., 1989). Throughout this report, "size" is the radius of the equivalent sphere reconstructed from the section of crystal. Olivine, pyroxenes and larger plagioclase crystals are almost equant grains and this approximation does not introduce any bias in CSD estimation. For the smallest plagioclase crystals, that are more elongated, this can introduce some underestimate in the size that could produce a slight decrease in the slope of CSD (Armienti et al., 1994); this effect is however negligible for elongation ratios less than 1:3 as observed in these crystals.

CSDs were collected on digitised images of thin sections in which single kinds of grains of interest (plagioclase, olivine, clinopyroxene and vesicles) were separated from the background. Digitisation of binary images of vesicles was performed by an image acquisition system and VISILOG software, mounted on a PC connected to a microscope for optical mineralogy. Binary images of olivine, clinopyroxene, plagioclase were acquired by hand contouring of photographs of thin sections (typically 21×30 cm corresponding to a matrix of 1216×1730 pixels), this allows one to separate crystals in glomerophyric aggregates. On selected samples binary images of plagioclase were also obtained combining digitised X-ray maps of elements, taken with an EDS microanalyser (LINK ExL equipped with FEATURE SCAN) linked to a Cambridge Stereoscan360 SEM. This procedure takes much longer and was used to test the reproducibility of the acquisition by hand contouring. Control samples indicate perfect agreement between plagioclase CSDs detected with the two methods (Armienti et al., 1994). On lava samples of 2002–2003, binary images of plagioclase crystals were obtained through automatic procedures based on the acquisition of several images collected in natural light and with crossed polars. This updated procedure allows the quick collection of larger data sets (Table 1), limiting the right-hand and left-hand truncation effects (Tarquini and Armienti, 2003).

The computation of grain characteristics (number, equivalent radius, area, elongation) and the reconstruction of crystal size distributions was performed by a technique (Pareschi et al., 1990) which derives crystal size distribution in the volume from digitised maps by using the Schwartz–Saltikov unfolding algorithm (DeHoff and Rhines, 1972). Resolution of the scanned images allows accurate detection of crystals larger than about 0.2 mm, thus avoiding the incorporation of groundmass crystals. CSD data have been computed by eliminating the effects of vesicularity on each sample. Data on vesicularity, investigated area and number of crystals detected in each sample are reported in Table 1. The mean area to investigate in order to obtain statistically significant data given by

$$A = \frac{1}{2\exp(n(L))\Delta L\sqrt{L\Delta L}} \quad (1)$$

Armienti et al. (1994) were A is the area of the section, $n(L)$ the number density of the particle of size L and ΔL is

UNCORRECTED PROOF

ARTICLE IN PRESS

t2.1 Table 2
t2.2 Slopes ($m=-1/G\tau$) and intercepts of plagioclase CSDs

t2.3 Sample	Slope	Ln n_o
t2.4 str45	−6.72	5.54
t2.5 str7-94	−6.60	5.33
t2.6 str9-94-B1	−6.44	5.40
t2.7 str9-94-B2	−7.50	5.83
t2.8 str09-94-A	−7.88	6.01
t2.9 str95a(03/95a)	−7.91	6.00
t2.10 str95b(03/95b)	−8.55	6.12
t2.11 str95c(03/95c)	−8.06	6.10
t2.12 str07-95(2)	−7.70	5.95
t2.13 str08-95 b(1)	−7.20	5.54
t2.14 str08-95-a(1)	−7.16	5.30
t2.15 str08-95-a(2) *	−9.06	12.96
t2.16 str07-95(1)	−8.17	6.06
t2.17 str09-95 a(1)	−8.39	6.22
t2.18 str09-95 a(2)	−7.83	5.94
t2.19 str09-95 b	−7.62	5.97
t2.20 str09-95 c(1)	−8.65	6.19
t2.21 str09-95 c(2)	−7.87	5.70
t2.22 str09-95-b(2)	−7.66	6.03
t2.23 str04-96 a1	−7.56	5.69
t2.24 str04-96 a2	−7.36	5.88
t2.25 str04-96 b	−8.05	6.00
t2.26 str08-96 b	−6.75	5.31
t2.27 str09-96	−8.61	6.32
t2.28 str09-96 a	−8.84	6.38
t2.29 str09-96 b1	−7.10	5.42
t2.30 str09-96 b2	−7.59	5.68
t2.31 str09-96 e1	−7.89	5.97
t2.32 str09-96 f1	−8.33	5.93
t2.33 str09-96 f2	−7.64	5.66
t2.34 str09-96 h	−7.24	5.44
t2.35 str09-96 l	−6.88	5.18
t2.36 str09-96-i	−7.60	5.64
t2.37 str09-96-j	−7.22	5.59
t2.38 str09-96-k	−7.97	5.89
t2.39 STR29.12.02	−7.01	5.20
t2.40 STR15.01.03	−6.66	5.19
t2.41 STR26.06.03	−7.25	5.36
t2.42 Average:	−7.62±0.62	5.76±0.34

t2.43 The mean is calculated for the period July 1994–September 1996 (averages±1σ).
t2.44 Samples str45 is not included in the mean.
t2.45 * Outlier at the significance level of 10%.

the resolution of the acquisition procedure. The area typically investigated on each thin section is about 6 cm^2 (purged of 25–50% of vesicularity, see Table 1): on the basis of Eq. (1) this guarantees, in most cases, the statistical reliability of plagioclase CSDs for each sample, up to sizes of about 1.2 mm. Larger crystals would have required an investigated area larger than was available. Thus for larger crystals statistical reliability was increased considering numerical values of CSDs in the context the total area (≈200 cm^2) of the whole set of measured thin sections.

3.2. Crystal balance equations

Crystal size distributions are suitable for a kinetic interpretation of crystallization processes since the number of crystals and the size they can reach depend on the cooling history; magmas are in fact populated by a number of crystals whose size changes according to the time of appearance (Dowty, 1980). Peaks in the size distribution ~~function~~ indicate a burst in the nucleation (expected for high undercooling ΔT), while flat distributions (about the same number of crystals of each size) suggest a nucleation occurring at constant undercooling (Kirkpatrick, 1977; Maaloe et al., 1989; Armienti et al., 1994). These behaviours can be explained on the basis of the balance equation (Marsh, 1988) for the number n of crystals per unit size per unit volume:

$$\frac{\partial Vn}{\partial t}+\frac{\partial GVn}{\partial L}=Q_{in}\,n_{in}-Q_{out}n_{out} \quad (2)$$

where t is time, L is crystal size, V is the volume of the magma, G is the crystal growth rate, Q is the magma flux rate (V/t), and Q_{in} and Q_{out} are respectively the crystal

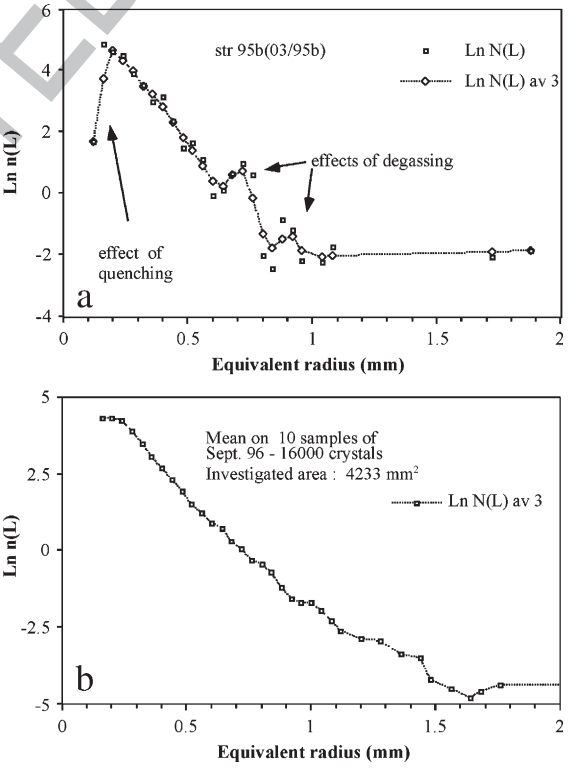


Fig. 4. (a) Effects of quenching and degassing on single CSDs. See text. (b) Cumulative plagioclase CSD for ten samples of September 1996. The larger total area of the cumulative sample allow us to report on the same linear distribution crystals up to 1.7 mm. A crystal larger than 2 mm is still out of range.

UNCORRECTED PROOF

ARTICLE IN PRESS

influx and outflow from the system. Eq. (2) simply states that, in the unit volume, the number of crystals of size between L and $L+\Delta L$ that appears in the unit time is provided by the number of crystals which acquire a given size due to growth from the lower class and growth in the larger class. The second member of Eq. (2) provides balance for a possible net flux of crystals of given size, added from an external source (Q_{in}) or lost in a sink (Q_{out}).

Eq. (2) can be solved under a variety of boundary conditions that rely on different hypotheses regarding the behaviour of the system and the dependence of growth and nucleation rates from size. For a magma chamber of constant size continuously filled and tapped ($Q_{in}=Q_{out}$) in which the input magma is crystal-free ($Q_{in}n_{in}=0$) and the output Q is given by V/τ where τ is the recharge time of the system, Marsh (1988) proposes the following solution:

$$n = n_o \exp(-L/G\tau) \text{ or else } : \ln(n) = \ln(n_o) - L/G\tau \quad (3)$$

which is based on the further assumption that crystal growth rate is independent of size L.

Eq. (3) describes the size distribution in a continuously-filled continuously-tapped magmatic system of constant size (RFT) in which crystals are lost only due to eruptions. On the basis of geochemical evidence these conditions seem to properly describe the behaviour of Stromboli and Eq. (3) will be used in the following to describe size distributions measurements on that volcano. According to Eq. (3) a plot in a semi-logarithmic diagram of Ln(n) vs. the size of the class provides linear trends in which the slope is proportional to $-1/G\tau$ and the intercept on y axis yields the nucleation rate (Marsh, 1988). If residence time or growth rates are known, the slope of the size distribution allows the estimate of the other variable; if both variables are known Eq. (3) allows assessment of the volume of the system by using estimates of magma output rates.

4. Measured CSDs

4.1. Plagioclase

A selection of typical CSDs is reported in Fig. 3, all the relevant data (slope and intercepts) are given in Table 2. In general all the distributions exhibit the same shape: they are linear in the size interval 0.2–12 mm, even if some samples have evident maxima (e.g. STR 95b.03-95b) in different size intervals (Fig. 4a). Crystals whose equivalent radius is larger than 1.2 mm seem to lay on a different trend, but in most cases this is an artefact due to the circumstance that conditions stated in Eq. (1) are not fulfilled. This can be clearly seen in the cumulative

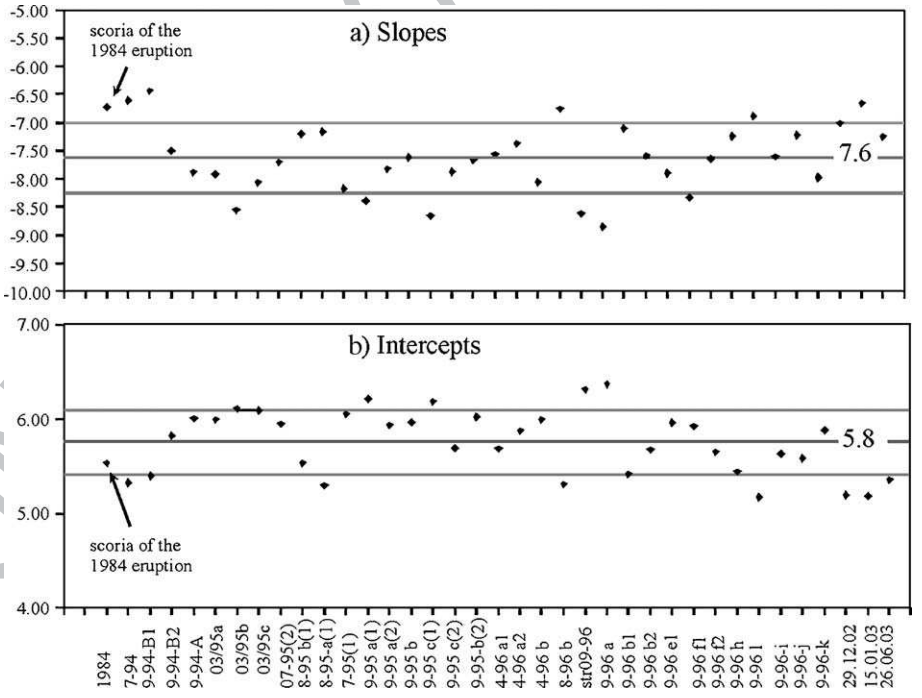


Fig. 5. Temporal variations of slopes (a) and intercepts (b) of plagioclase CSDs in Stromboli scoriae from April 1994 to September 1996. CSDs measured for the eruptions of 1984 and 2002–2003 are within the standard deviation of 1994–96 CSD data. In grey $\pm 1\sigma$ confidence intervals.

ARTICLE IN PRESS

diagram of Fig. 4b, where all eleven samples of September 1996 are considered as a single data set and the larger crystals lay on the same trend of smaller ones. This effect is due to the poor count statistics of larger crystal (right hand truncation effect). The largest plagioclases of this data set are cognate xenocrysts entrapped from the conduit walls and do not lay on the linear trend. Crystals smaller than 0.2 mm show a pronounced decrease of their number density in all the scoriae in which crystal were hand contoured (Fig. 4a, *effect of quenching*), this is mainly an artifact arising from the detection limit of the acquisition technique. The higher resolution attainable with the automatic procedure shifts the left-hand truncation effect down to size of 0.06 mm (Fig. 4b).

The above considerations allow to show that the size interval 0.2–1.2 mm is significant for the following discussion due to the absence of both right and left hand truncation effects (Armienti and Tarquini, 2002). Fig. 5 (a,b) displays the temporal variation of slopes and intercepts of the linear CSDs in the size interval 0.2–1.2 mm revealing a striking constancy of both parameters within 1σ confidence interval with the exception of sample str09-95-b(2) (not reported in Fig. 5) that is considered an outlier. The same values are also displayed by older samples (1984, shown by comparison in the same figures) within 1σ confidence limit. The average values of slope and intercepts of linear trends are -7.69 (± 0.60) ($N*1^{-5}$ and 5.80 (± 0.32 $N*1^{-3}$), respectively. Our data set reveal that, at the gross scale, the conditions in which plagioclase CSDs are formed at Stromboli are constant in the past two decades and reinforce observation arising from volcanological, petrological and geochemical considerations about the stationary state characterising this volcanic system. However, at the fine scale, within the 1σ variability of the data set, a kind of cyclic behaviour to both CSD slopes and intercepts can be figured out. It can be tentatively related to the dynamics of the recharge system, but a more finely spaced temporal series would be necessary for a well sound interpretation.

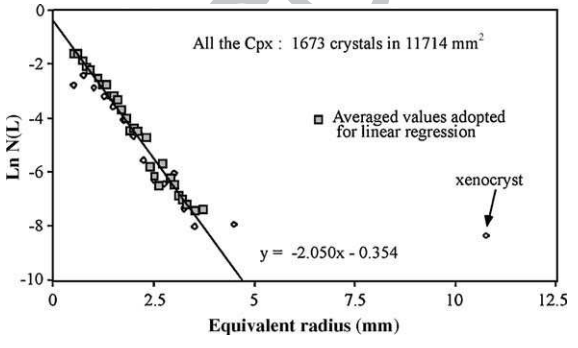


Fig. 6. Cumulative diagram of clinopyroxene CSDs for the data set of Table 1. Regression parameters of the linear trend are given in the figure. The larger crystal not lying on the linear trend is probably a xenocryst.

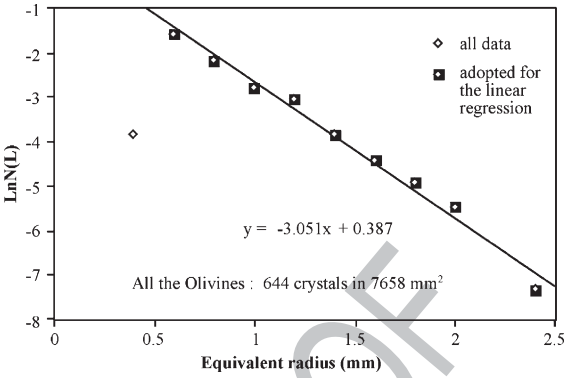


Fig. 7. Cumulative diagram of Olivine CSDs for the data set of Table 1. Regression parameters of the linear trend are given in the figure.

5. Clinopyroxene and olivine

Pyroxene and olivine grains occurring in a single thin section were not in sufficient amount to statistically fulfil the conditions required from Eq. (1). However, the constant behavior revealed by plagioclase CSDs allows us to consider the entire population of mafic crystals as a single sample representative of the main (and practically) constant behaviour of the system. In Figs. 6 and 7 CSD data of mafic phases are reported for samples of the period April 1994–September 1996 and reveal the same linear trends that characterise plagioclase CSDs. For pyroxene the slope of the total linear distribution is -2.05 and the intercept is 0.35 for olivine the two values are -3.05 and 0.39, respectively.

6. Discussion

The uniform eruptive regime, constant slopes and intercepts of CSDs, mineralogical and geochemical data suggest that Stromboli volcano is in a steady-state condition. In particular, geochemical modeling (Francalanci et al., 1999, 2004; Landi et al., 2004) suggests a condition of continuous refilling, mixing, crystallisation and eruption of magma which fully satisfies the description of a crystallizator system for which Marsh (1988) proposed a solution for the crystal balance equation (Eq. (2)). This allows us to use Eq. (3) to safely extract temporal information from crystal size distribution slopes. It is important to note that the seriated texture of Stromboli scoriae result in CSDs completely lacking the curvatures and kinks commonly found in other volcanoes and associated to porphyritic textures

CORRECTED PROOF

ARTICLE IN PRESS

(Fig. 8) (Marsh, 1988; Cashman, 1988; Mangan, 1990; Cashman, 1992; Armienti et al., 1994; Zieg and Marsh, 2002). Minor maxima found in some plagioclase CSDs can be preserved in the final scoriae due to incomplete mingling of HP magma with LP magma in coherent regions (Perugini and Poli, 2000) that prevents resorption, and consequent consumption, of smallest crystals. These can become later available for further growth, leaving the fingerprint of a relative maximum in CSDs. Sporadic maxima in nucleation and growth are, ultimately, the effects of degassing that strongly affects nucleation and growths rates (Armienti et al., 1994; Simakin et al., 1998; Landi et al., 2004).

6.1. Plagioclase CSDs

Mineral growth rates can be estimated, if residence time is known, on the basis of the equation $m = -1/G\tau$, where m is the slope of CSDs.

The residence time of Stromboli shallow feeding system has been estimated to be 19 years on the basis of Sr isotopic data (Francalanci et al., 1999). This estimate of residence time would imply a plagioclase growth rate on the order of 2×10^{-11} cm s^{-1}. This seems too low considering the results obtained on basaltic systems, on average in the range 10^{-9}–10^{-10} cm s^{-1} (Kirkpatrick et al., 1976; Lofgren, 1980; Armienti et al., 1994). However the obtained low growth rate of the plagioclase is the result of an average behaviour which must account for the peculiar textural and chemical zoning of the plagioclase. Indeed, plagioclase crystals in the crystal-rich scoriae, show alternating layers of labradoritic and bytownitic composition, that allow one to recognize distinct recurrent phases of growth and dissolution (Landi et al., 2004). Thus we can assume that the growth rate G derived from CSD data is a mean resulting from growth and dissolution episodes.

$$\bar{G} = G^{+}f^{+} + G^{-}f^{-} \tag{4}$$

where G^{+} and G^{-} are mean growth and dissolution rates, respectively, and f^{+} and f^{-} are the volume fractions of the system in which crystals grow or dissolve respectively. For a system that behaves like a crystallizing system, we can assume f^{+} to be proportional to the volume fraction of magma supplied in a characteristic time:

$$f^{+} = (V - Q^{*}\Delta t)/V \tag{5}$$

where Q is the magma supply rate, which, in a steady system, is equal to the mass eruption rate and Δt is a characteristic time during which resorption events may occur due to mixing of undegassed LP magma with the resident HP magma.

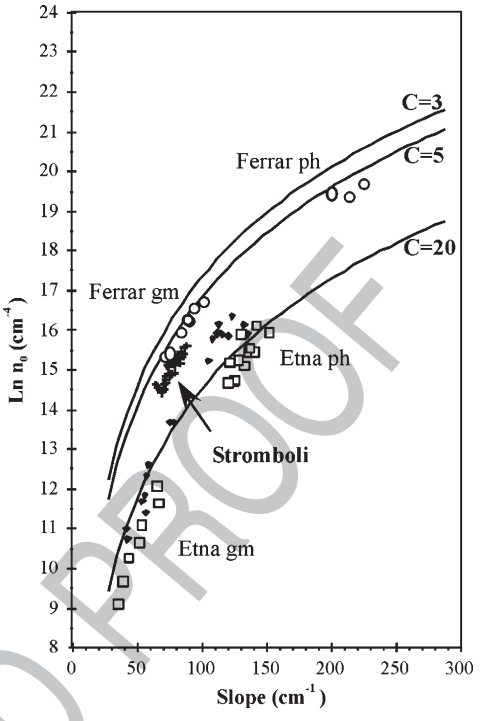


Fig. 8. Plot of CSD intercepts vs. slopes according to the dimensional analysis of Zieg and Marsh (2002). Porphyritic lavas of 2001 eruptions of Mt. Etna and Ferrar dolerites are plotted with seriated Stromboli scoriae. The porphyritic structure implies the adoption of different linear regressions for phenocrystals (ph) and groundmasses (gm) that is reflected by distinct grouping of CSD data for Etna and Ferrar. For Stromboli each CSD can be regressed by a single linear relations resulting in a single cluster of data. Source of data — Etna: 2001 eruption, from distinct eruptive fractures (diamonds and squares, Armienti unpublished data). Ferrar dolerites from Zieg and Marsh (2002). Stromboli, Table 2. The curves represent the theoretical relation $\mathrm{Ln}(n_o) = 4\,\mathrm{Ln}(\mathrm{slope}) - \mathrm{Ln}\,C$ (Eq. (19) of Zieg and Marsh, 2002) where C is related to different crystallinity : C=3 plg=70 vol.%; C=5 plg=42 vol.%; C=20 plg=8 vol.%.

From the obvious relations $f^{+}+f^{-}=1$ and $V/Q=\tau$, it follows:

$$f^{+} = 1-\Delta t/\tau \text{ and } f^{-} = \Delta t/\tau \tag{6}$$

thus:

$$\bar{G} = G^{+}\left(1-\frac{\Delta t}{\tau}\right) + \bar{G}\left(\frac{\Delta t}{\tau}\right) \tag{7}$$

which states that the net growth rate is a mean of positive and negative growth rates weighted for the times in which the two conditions hold.

The internal consistency of Crystal Size Distribution and residence times based on isotopic disequilibria may

UNCORRECTED PROOF

ARTICLE IN PRESS

be assessed by means of the above equation. Assigning different values for G^+, the value of G^- may be computed from Eq. (7)) for different choices of Δt. In correspondence with these characteristic times of dissolution we can compute the amount of dissolution allowed for crystals ($G^- * \Delta t$). Thus a plot ~~($-G^- * \Delta t$)~~ vs. ~~$-\Delta t/\tau$~~ for different G^+, will provide~~,~~ an estimate of the characteristic size of the crystal that will be completely resorbed. It is worth noting that crystals, with sizes smaller than the amount of dissolution allowed, will not show resorption features in so far they are completely consumed during this phase. The graph of Fig. 9 shows that for $\bar{G}=10^{-8}$ cm/s crystals of centimetre size would be completely resorbed, thus it would be impossible to observe any resorption features in phenocrysts less than 1 cm in diameter. For $\bar{G}=10^{-9}$ cm/s for most of $\Delta t/\tau$ values, crystals of about 1 cm would be resorbed and to resorb only millimetric crystals the volume fraction in which the process should take place would be too large (about 1). Thus, since only crystals in the size range of a few hundreds of μm do not show resorptions an order of magnitude of $G^+=10^{-10}$ cm/s must be assumed for plagioclase growth rates in the Stromboli feeder conduit.

This mechanism implies that also the plagioclase nucleation rates result from a mean behaviour of the system and that the observed intercepts of CSDs are the balance of resorptions and nucleation bursts.

6.2. Mafic phases

These details of the crystallisation process cannot be observed for mafic phases due to the insufficient size of each sample for statistically reliable CSDs. When considering sets of samples obtained by grouping scoriae of a longer period, however, the uniform behaviour of the system still emerges.

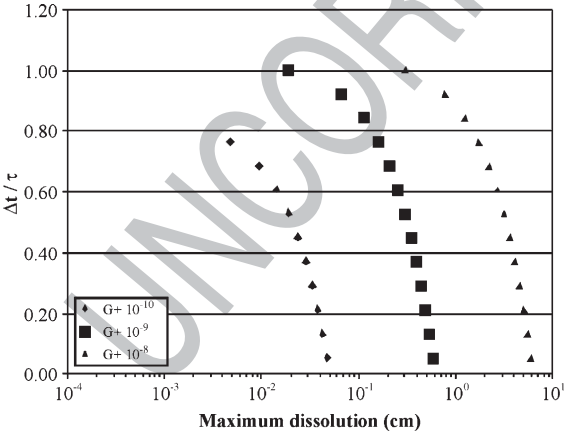


Fig. 9. Plot of $\Delta t/\tau$ vs. $-G^*\Delta t$ from Eq. (7). The diagram provides the maximum size of crystals that can be completely resorbed for given values of $\Delta t/\tau$. $\tau=19$ years and different values for plagioclase growth rate. See text for major details.

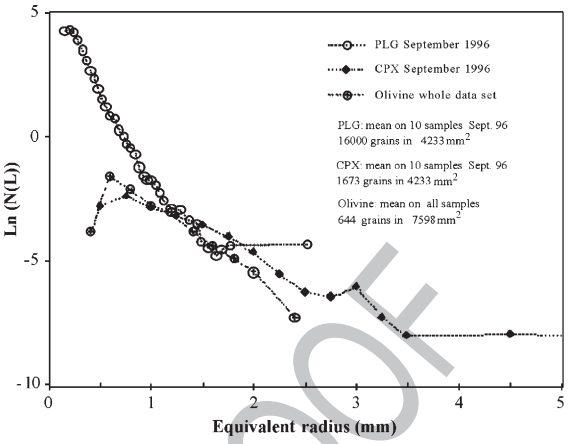


Fig. 10. Comparison of CSDs for plagioclase, olivine and clinopyroxene of comparable periods (September 1996). Linear regression on the three data set yields the following values: Plagioclase: Ln $n(L)=-7.69L+5.80$. Clinopyroxene: Ln $n(L)=-1.72L-1.30$. Olivine: Ln $n(L)=-3.05L+0.38$.

Fig. 10 compares CSDs of plagioclase, clinopyroxene and olivine of September 1996. They all show linear trends confirming that all the crystal content of Stromboli products forms with the same mechanism. This reinforces the conclusion that Stromboli is continuously supplied by a LP magma that assumes its stationary HP composition and crystallinity due to mechanisms of continuous refilling, mixing, crystallisation and sampling due to eruptions. For the investigated period the values of slopes of linear distribution for the three examined minerals are in the ratio:

$$m_{pl} : m_{ol} : m_{cpx} = 7.69 : 3.05 : 2.05$$

since the same mechanism acts on each kind of crystals, this means that they form in the same characteristic time of recharge of the system (τ of Eq. (3)) and consequently on the basis of the relations between CSD slopes and growth rates ($m=1/G\tau$), growth rates are in inverse relation. If plagioclase growth rate is assumed equal to 1 mineral growth rates must keep the ratios:

$$G_{pl} : G_{ol} : G_{cpx} = 1 : 2.5 : 3.7$$

this means that in the Stromboli feeding system olivine and clinopyroxene grow more than two and almost four time faster than plagioclase, respectively.

With the mean growth rate of the plagioclase we can estimate $G_{ol} \sim 2.5*10^{-11}$ cm s^{-1} and $G_{cpx} \sim 3.7*10^{-11}$ cm s^{-1}.

UNCORRECTED PROOF

ARTICLE IN PRESS

These low values also suggest that mafic phases undergo resorption episodes that can be revealed in clinopyroxenes by the widespread occurrence of resorbed diopsidic zone.

7. Conclusions

Stromboli is a stationary system which behaves like a crystallizing system, it is a rare natural system fulfilling the Eq. (3).

The residence time of 19 years and the slopes of CSD imply a mean growth rate of plagioclase of $2 * 10^{-11}$ cm/s which is smaller than values reported in literature. The occurrence of resorptions allows to an assessment of balance between growth and dissolution episodes. Thus net growth rate results to be 10^{-10} cm/s. Resorptions in plagioclase crystal continuously reduce the number of crystal nuclei and necessarily play a major role in the formation of the seriated structure of Stromboli scoriae as well as in the stationary systems that exhibit seriated structures. Even if a different estimate of the magma residence time derived from Sr isotopic data may affect the numerical value of growth rates, the model is robust in explaining both the occurrence of resorption features of larger crystal and the lack of these effects in crystals smaller than a few hundreds of micrometers.

Crystal size distribution data of scoriae emitted at Stromboli in the time span 1994–2003 can be interpreted on the basis of equation Ln $n(L) = -L/G\tau + \mathrm{Ln}\ (n_o)$ that allows to estimate magma residence time and nucleation rates for the different phases. CSDs for plagioclase, olivine and pyroxene are practically constant in the examined time span and controls on older samples allow us to conclude that this volcano has been keeping a constant behaviour in the last decades being practically in stationary conditions. Local maxima sporadically observed in some plagioclase CSD are interpreted as due to incomplete homogeneity of portions of HP magma. The linear CSDs typical of all the phases confirm the crystallisation of Stromboli magma takes place in a stationary crystallising system continuously filled by crystal-free supply of basaltic melt. Growth rates of minerals are in the ratio

$$G_{plg} : G_{ol} : G_{cpx} = 1 : 2.5 : 3.7$$

8. Uncited references

Francalanci, 1993

Pikering et al., 1995

Acknowledgements

This work has been performed by the financial support of MIUR 2004 grant "Cinetiche di cristallizzazione e scale temporali dei processi magmatici come testimoniati dalle tessiture delle rocce vulcaniche: studi sperimentali e teorici ed osservazioni" (Pisa unit, issued to P.A.), INGV–GNV and the European Commission of Energy, Environment and Sustainable Development, through ERUPT project (EVG1-CT2002-00058), issued to L.F.

We wish to thank K. Cashman for her critical review of a preliminary version of the manuscript.

References

Allard, P., Carbonelle, J., Métrich, N., Loyer, H., Zettwoog, P., 1994. Sulphur output and magma degassing budget of Stromboli volcano. Nature 368, 326–330.

Armienti, P., Tarquini, S., 2002. Power-law olivine crystal size distributions in lithospheric mantle xenoliths. Lithos 64 (3–4), 273–285.

Armienti, P., Pareschi, M.T., Innocenti, F., Pompilio, M., 1994. Effects of magma storage and ascent on the kinetics of crystal growth. The case of 1991–93 Mt. Etna eruption. Contrib. Mineral. Petrol. 115, 402–414.

Barberi, F., Rosi, M., Sodi, A., 1993. Volcanic hazard assessment at Stromboli based on review of historical data. Acta Vulcanol. 3, 173–187.

Bertagnini, A., Coltelli, M., Landi, P., Pompilio, M., Rosi, M., 1999. Violent explosions yield new insights into dynamic of Stromboli volcano. EOS Trans. AGU 80 (52), 633–636.

Bertagnini, A., Métrich, N., Landi, P., Rosi, M., 2003. Stromboli an open window on the deep feeding system of a steady state volcano. J. Geophys. Res. 108 (B7), 2336, doi:10.1029/2002JB002146.

Bonaccorso, A., Cardaci, C., Coltelli, M., Del Carlo, P., Falsaperla, S., Panucci, S., Pompilio, M., Villari, L., 1996. Annual report of the world volcanic eruptions in 1993 Stromboli. Bull. Volcan. Erupt. 33, 7–13.

Cashman, K.V., 1988. Crystallisation of Mount St. Helens 1980–1986 dacite: a quantitative textural approach. Bull. Volcanol. 50, 194–209.

Cashman, K.V., 1992. Groundmass crystallization of Mount St. Helens dacite 1980–1986: a tool for interpreting shallow magmatic processes. Contrib. Mineral. Petrol. 109, 431–449.

Cashman, K.V., Marsh, B.M., 1988. Crystal size distribution (CSD) in rocks and the kinetics and dynamics of crystallization II: Makaopuhi lava lake. Contib. Mineral. Petrol. 99, 292–305.

DeHoff, R.T., Rhines, F.N., 1972. Microscopie Quantitative. Masson et Cie, Paris, p. 404.

Dowty, E., 1980. Crystal growth and nucleation theory and numerical simulation of igneous crystallization. In: Hargraves, R.B. (Ed.), Physics of Magmatic Processes. Princeton University Press, pp. 385–417.

Francalanci, L., 1993. Mineral chemistry of Stromboli volcanics as indicator of magmatic processes. Acta Vulcanol. 3, 99–113.

Francalanci, L., Manetti, P., Peccerillo, A., Keller, J., 1993. Magmatological evolution of the Stromboli volcano (Aeolian Arc, Italy): inferences from major and trace element and Sr-isotopic composition of lavas and pyroclastic rocks. Acta Vulcanol. 3, 127–151.

UNCORRECTED PROOF

ARTICLE IN PRESS

Francalanci, L., Tommasini, S., Conticelli, S., Davies, G.R., 1999. Sr isotope evidence for short magma residence time for the 20th century activity at Stromboli volcano Italy. Earth Planet. Sci. Lett. 167, 61–69.

Francalanci, L., Tommasini, S., Conticelli, S., 2004. The volcanic activity of Stromboli in the 1906–1998 AD period: mineralogical, geochemical and isotopic data relevant to understanding of the plumbing system. J. Volcanol. Geotherm. Res. 131, 179–211.

Francalanci, L., Davies, G.R., Lustenmhower, W., Tommasini, S., Mason, P., Conticelli, S., 2005. Intra-grain Sr isotope evidence for crystal re-cycling and multiple magma reservoirs in the recent activity of Stromboli volcano, southern Italy. J. Petrol.doi:10.1093/petrology/egi045

Giberti, G., Jaupart, C., Sartoris, G., 1992. Steady-state operation of Stromboli volcano, Italy: constraints on the feeding system. Bull. Volcanol. 54, 535–541.

Harris, A.J.L., Stevenson, D.S., 1997. Magma budgets and steady state activity of Vulcano and Stromboli. Geophys. Res. Lett. 24, 1043–1046.

Kirkpatrick, R.J., 1977. Nucleation and growth of plagioclase, Makaopuhi and Alae lava lakes Kilauea Volcano, Hawaii. Geol. Soc. Am. Bull. 88, 78–84.

Kirkpatrick, R.J., Gilpin, R.R., Hays, J.F., 1976. Kinetics of crystal growth from silicate melts: anorthite and diopside. J. Geophys. Res. 81, 5715–5720.

Landi, P., Métrich, N., Bertagnini, A., Rosi, M., 2004. Dynamics of magma mixing and degassing recorded in plagioclase at Stromboli (Aeolian Archipelago Italy). Contrib. Mineral. Petrol. 147, 213–237.

Lofgren, G.E., 1980. Experimental studies on the dynamic crystallization of silicate melts. In: Hargraves, R.B. (Ed.), Physics of Magmatic Processes. Princeton University Press, pp. 487–551.

Maaloe, S., Tumyr, O., James, D., 1989. Population density and zoning of olivine phenocrysts in tholeiites from Kauai, Hawaii. Contrib. Mineral. Petrol. 101, 176–186.

Mangan, M.T., 1990. Crystal size distribution systematics and the determination of magma storage times: the 1959 eruption of Kilauea volcano, Hawaii. J. Volcanol. Geotherm. Res. 44, 295–302.

Marsh, D.B., 1988. Crystal size distribution (CSD) in rocks and the kinetics and dynamics of crystallisation I. Theory. Contrib. Mineral. Petrol. 99, 277–291.

Métrich, N., Bertagnini, A., Landi, P., Rosi, M., 2001. Crystallisation driven by decompression and water loss at Stromboli volcano (Aeolian Islands). J. Petrol. 42 (8), 1471–1490.

Pareschi, M.T., Pompilio, M., Innocenti, F., 1990. Automated evaluation of volumetric grain-size distribution density from thin-section images. Comp. Geosci. 16, 1067–1084.

Perugini, D., Poli, G., 2000. Chaotic dynamics and fractals in magmatic interaction processes: a different approach to the interpretation of mafic microgranular enclaves. Earth Planet. Sci. Lett. 175, 93–103.

Pikering, G., Bull, J.M., Sanderson, D.J., 1995. Sampling power_law distributions. Tectonophysics 248, 1–20.

Rosi, M., Bertagnini, A., Landi, P., 2000. Onset of the persistent activity at Stromboli volcano (Italy). Bull. Volcanol. 62, 294–300.

Simakin, A.G., Armienti, P., Epel'baum, M.B., 1998. Coupled degassing and crystallization: experimental study in continuous pressure drop, with application to volcanic bombs. Bull. Volcanol. 61, 275–287.

Tarquini, S., Armienti, P., 2003. Quick determination of crystal size distributions of rocks by means of a color scanner. Image Anal. Stereol. 22, 27–34.

Vagelli, G., Francalanci, L., Ruggirei, G., Testi, S., 2003. Persistent polybaric rests of calc-alkaline magmas at Stromboli volcano, Italy: pressure data from fluid inclusions in restitic quartzite nodules. Bull. Volcanol. 65, 385–404.

Zieg, M.J., Marsh, B.D., 2002. Crystal size distributions and scaling laws in the quantification of igneous textures. J. Petrol. 43, 85–101.

UNCORRECTED PROOF